PHYSICAL REVIEW B VOLUME 43, NUMBER 1 1 JANUARY 1991

Optical conductivity in high-T_c superconductors

E. J. Nicol, J. P. Carbotte, and T. Timusk
Physics Department, McMaster University, Hamilton, Ontario, Canada L8S 4M1
(Received 9 July 1990)

The optical conductivity of a superconductor with arbitrary mean free path is calculated with use of an imaginary-frequency formulation. We obtain good agreement with the results of a recent real-axis formulation and, in most cases, with another imaginary-frequency formulation. Extending the work to a simple version of a recently proposed phenomenological charge-transfer resonance model for the CuO, it is found that in the clean limit the absorption will start at four times the gap (Δ_0) while introducing impurities produces absorption starting at twice Δ_0. In agreement with experiment, strong coupling effects at higher energies need not be large in this model.

I. INTRODUCTION

Infrared measurements on superconductors can yield important information on the excitation spectrum of the system in the energy range of a few times the energy gap Δ_0, and are therefore very important. Because of this, many experimental studies on the high-T_c oxides have now been published. These are too numerous to describe here and the reader is referred to the recent review of Timusk and Tanner for references and discussion.[1] While there is, at present, a great deal of agreement among the various researchers as to experimental results, their interpretation remains controversial.[2,3] While some authors argue for the existence of a large gap $2\Delta_0/k_BT_c \sim 8$,[2] others reason that a gap cannot be seen in the clean limit.[3] At higher energies the exact nature of the mid-infrared absorption is also not yet known.[3]

Recently, Lee, Rainer, and Zimmermann[4] have given a real-frequency formulation of the optical conductivity, valid for any value of the mean free path. They have studied, within such a formalism, several possible models for the Eliashberg kernels which could possibly be applicable to the high-T_c oxides. They give results for pure phonon as well as combined phonon-plus-exciton models with particular emphasis placed on the Holstein effect. These processes reflect some of the details of the excitation spectrum involved. Complementary calculations using an imaginary-frequency-axis (Matsubara) formulation of the theory with final analytic continuation of the current-current correlation function using Padé approximants have been performed by Bickers *et al.*[5] These conventional strong-coupling calculations predict large changes in the infrared spectrum in the Holstein region when the materials become superconducting. There is general agreement among experimentalists that such structures are not observed in the infrared conductivity.[3,6]

In this paper we present numerical results using the imaginary-axis formulation for the current-current correlation function. After verifying our work against known results and pointing out a discrepancy with a recent calculation, we generalize the work to include both charge- and spin-fluctuation channels. To illustrate the effects that are then possible, we use a simple version of a recently proposed marginal Fermi-liquid model,[7-11] which is based on a phenomenological charge-transfer resonance model and may be applicable to the CuO. In this model the coupling to charge and spin degrees of freedom is described by the same excitation spectrum but with different coupling strength. Such a model is formally described by the same mathematical equations as for phonons plus paramagnons[12-14] with the difference that now the Eliashberg kernels are temperature dependent.

In Sec. II we summarize, without derivation, the necessary formalism while in Sec. III, a comparison with results of other work is given. The phenomenological charge-transfer resonance model is treated explicitly in Sec. IV for arbitrary mean free path values. A short conclusion is found in Sec. V.

II. FORMALISM

The conductivity $\sigma(\omega)$ is related to the real-frequency-axis analytic continuation of the current-current correlation function $\Pi(i\nu_m)$ which is known, within a Matsubara formalism, only at discrete boson frequencies $\nu_m = 2m\pi T$ where m is an integer and T is the temperature. Specifically,

$$\sigma(\omega)=\frac{i}{\omega}\Pi(i\nu_m \rightarrow \omega + i0^+) \ . \tag{1}$$

Referring to Bickers *et al.*[5] for details, $\Pi(i\nu_m)$ is given in terms of the plasma frequency ω_p, the Matsubara gaps $\tilde{\Delta}_n$, and renormalization factors $\tilde{\omega}_n$ by

$$\Pi(i\nu_m)=\frac{\omega_p^2}{4\pi}\pi T\sum_n S_{n,m} \ , \tag{2}$$

with

$$S_{n,m}=\begin{cases}\dfrac{\tilde{\omega}_n(\tilde{\omega}_n+\tilde{\omega}_{n+m})+\tilde{\Delta}_n(\tilde{\Delta}_n-\tilde{\Delta}_{m+n})}{R_nP_{n,m}} & \\ -\dfrac{\tilde{\omega}_{n+m}(\tilde{\omega}_{n+m}+\tilde{\omega}_n)+\tilde{\Delta}_{n+m}(\tilde{\Delta}_{n+m}-\tilde{\Delta}_n)}{R_{n+m}P_{n,m}}, & \text{for } (m\neq 0,\ -2n-1) \quad (3a)\\ \tilde{\Delta}_n^2/R_n^3, \quad \text{for } (m=0) & (3b)\\ 1/R_n, \quad \text{for } (m=-2n-1)\ . & (3c)\end{cases}$$

In Eq. (3), $R_n=\sqrt{\tilde{\omega}_n^2+\tilde{\Delta}_n^2}$ and $P_{n,m}=\tilde{\omega}_n^2-\tilde{\omega}_{n+m}^2+\tilde{\Delta}_n^2-\tilde{\Delta}_{n+m}^2$.

The Matsubara gaps and renormalization functions are given by[15,16]

$$\tilde{\Delta}_n=\pi T\sum_m\lambda^-(m-n)\frac{\tilde{\Delta}_m}{\sqrt{\tilde{\omega}_m^2+\tilde{\Delta}_m^2}}+\pi t^+\frac{\tilde{\Delta}_n}{\sqrt{\tilde{\omega}_n^2+\tilde{\Delta}_n^2}} \quad (4)$$

and

$$\tilde{\omega}_n=\omega_n+\pi T\sum_m\lambda^+(m-n)\frac{\tilde{\omega}_m}{\sqrt{\tilde{\omega}_m^2+\tilde{\Delta}_m^2}}+\pi t^+\frac{\tilde{\omega}_n}{\sqrt{\tilde{\omega}_n^2+\Delta_n^2}}\ , \quad (5)$$

where $\omega_n=(2n+1)\pi T$ with $n=0,\pm1,\pm2,\ldots$, and $\pi t^+\equiv 1/(2\tau)$ with τ the residual scattering rate. In Eqs. (4) and (5) we have neglected the Coulomb pseudopotential and $\lambda(n-m)$ is given in terms of the electron–exchange-boson spectral density $\alpha^2F(\omega)$ for any boson exchange process of interest, i.e., phonons, plasmons, charge fluctuations, etc., by

$$\lambda^+=\lambda^-=\lambda(n-m)=\int_0^\infty\frac{2\omega\alpha^2F(\omega)}{\omega^2+(\omega_n-\omega_m)^2}d\omega\ . \quad (6)$$

In the marginal Fermi-liquid model,[7–11] an essential feature is the coupling to both charge and spin fluctuations as described by Kuroda and Varma.[11] In this case the charge degrees of freedom, which are pair creating, couple to the superconducting electrons through a dimensionless coupling λ_ρ while coupling to spin is described by λ_σ. The modifications of Eqs. (4) and (5) are made by replacing $\lambda^-(m-n)$ by $(\lambda_\rho-\lambda_\sigma)F(m-n)$ and $\lambda^+(m-n)$ by $(\lambda_\rho+\lambda_\sigma)F(m-n)$ where in a simple approximation

$$F(m-n)=\frac{1}{\pi}\int_0^{\omega_c}\frac{2\omega\tanh(\omega/2T)}{\omega^2+(\omega_m-\omega_n)^2}d\omega\ . \quad (7)$$

Here ω_c is an upper cutoff on the excitation spectrum. Also, as a superconducting gap (Δ_0) develops in the superconducting electron system, a lower cutoff of $2\Delta_0$ is to be applied as the lower limit in the integral. This is to be determined self-consistently. Note that, the parameters of the theory are λ_ρ, λ_σ, and ω_c. In presenting the results it is convenient to introduce instead $g\equiv(\lambda_\rho-\lambda_\sigma)/(\lambda_\rho+\lambda_\sigma)$ which describes the relative coupling to charge and spin and to fix λ_ρ to get a critical temperature value $T_c=100$ K as illustrative of the oxides. This leaves g and the upper cutoff ω_c as the only two parameters.

III. NUMERICAL RESULTS AND COMPARISON TO PREVIOUS WORK

The model used by Bickers *et al.*[5] for $\alpha^2F(\omega)$ is that of a single truncated Lorentzian with peak position at ω_0 and width Γ_0 and truncated at Γ_c, i.e.,

$$\alpha^2F(\omega)\propto\left[\frac{1}{(\omega-\omega_0)^2+\Gamma_0^2}-\frac{1}{\Gamma_c^2+\Gamma_0^2}\right],\quad |\omega-\omega_0|<\Gamma_c\ , \quad (8a)$$

$$\alpha^2F(\omega)=0,\quad |\omega-\omega_0|>\Gamma_c\ . \quad (8b)$$

The parameters are $\omega_0=50$ meV, $\Gamma_0=5$ meV, and $\Gamma_c=3\Gamma_0=15$ meV. In Fig. 1 we show our results for the

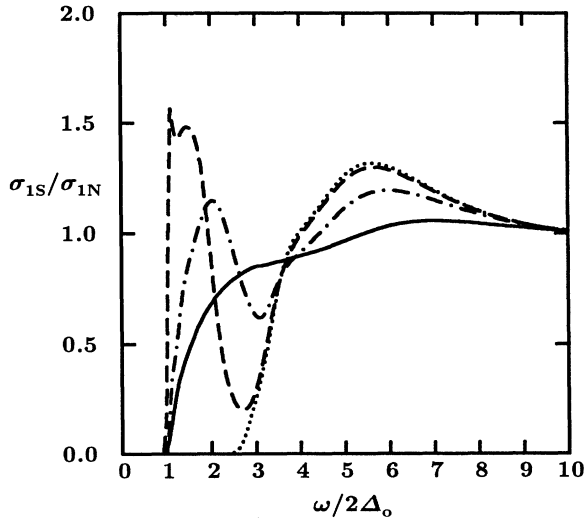

FIG. 1. The ratio of the real part of the conductivity in the superconducting state to that of the normal state as a function of frequency in units of twice the energy gap Δ_0. Four impurity concentrations are considered, as defined in the text. Except for the pure limit case, the results are in excellent agreement with those of Bickers *et al.* (Ref. 5) obtained for the same phonon model and using the same Matsubara formulation of the conductivity.

ratio of the real part of the conductivity in the superconducting state divided by the normal state $[\sigma_{1S}(\omega)/\sigma_{1N}(\omega)]$. The same four impurity concentrations, $t^+=0.0$ (dotted curve), 0.796 meV (dashed curve), 7.96 meV (dashed-dotted curve), and 79.6 meV (solid curve) as considered by Bickers *et al.*[5] are illustrated. These results are in excellent agreement with those of Bickers *et al.*[5] except for the dotted curve. In our case, the curve begins to rise at a value of twice the gap plus the first excitation energy in the phonon spectrum. This must be so physically, since we are in the clean limit. Bickers *et al.*[5] show only a pronounced dip at this energy and then absorption down to $2\Delta_0$ which cannot be correct and is probably an artifact of their analytic continuation technique[17] using Padé approximants. Except for the problem just mentioned, the excellent agreement for the other values of t^+ speaks to the correctness of the numerical techniques in both works.

It is of importance to compare the results obtained for the conductivity $\sigma(\omega)$ using the imaginary-axis formulation represented in Eqs. (1)–(5) with results of direct real-axis calculations. Such a formulation, for arbitrary impurity content $\pi t^+=1/(2\tau)$, has been considered recently by Lee, Rainer, and Zimmermann.[4] It involves formulas for $\sigma(\omega)$ that are mathematically very different from Eqs. (1)–(3) of the present paper and makes use of the real-frequency-axis version of the Eliashberg[18] equations instead of (4) and (5). These are much more complicated to solve numerically but no analytic continuation[17] is needed to obtain $\sigma(\omega)$ so that Padé approximants can be avoided entirely. In Fig. 2 we compare results obtained in this work (solid line) with the real-axis results of Lee, Rainer, and Zimmermann[4] (dashed line). The near exact agreement is impressive and gives us confidence to proceed and consider a marginal Fermi liquid in the next section. Note that the case considered in Fig. 2 is model *C* of Lee *et al.*[5] In this model a δ function model is used for the spectral density $\alpha^2F(\omega)$ with average phonon energy at 50 meV, the mass enhancement parameter $\lambda=0.8$, the plasma frequency is 820 meV, and the inverse scattering time is 1.05 meV with a T_c value of 50 K and a corresponding gap to critical temperature ratio, $2\Delta_0/k_BT_c$, of 3.9.

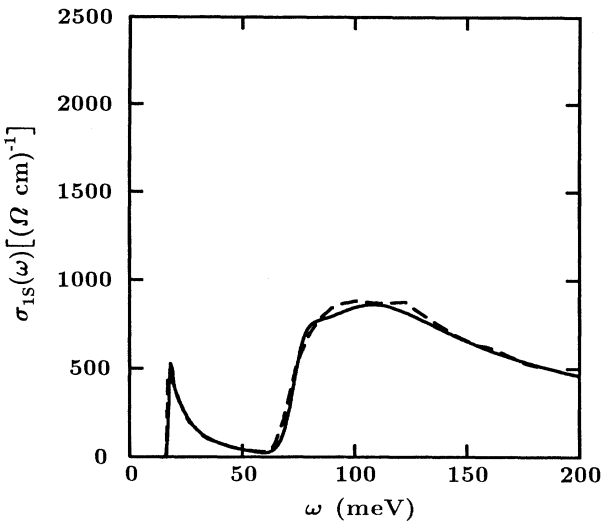

FIG. 2. A comparison of the real part of the conductivity in the superconducting state $\sigma_{1S}(\omega)$ in units of $(\Omega\ \mathrm{cm})^{-1}$ as a function of frequency ω in meV. The solid curve was obtained in this paper using the imaginary-frequency-axis formulation for the conductivity, namely, Eqs. (1)–(5). The dashed curve shown for comparison is the result of Lee *et al.* (Ref. 4) for their model *C*, defined in the text, which they obtained from a real-frequency-axis formulation. The agreement between the two methods is very good.

IV. RESULTS FOR MARGINAL FERMI-LIQUID MODEL

In all the results to be presented in this section, the critical temperature is fixed at 100 K. The two remaining parameters are the upper cutoff on the fluctuation spectrum ω_c [Eq. (7)] and the relative admixture of the coupling to charge and spin (g). First, we present a series of results for the clean limit ($t^+=0$) with $g=0.6$ as a function of cutoff ω_c. These are presented in Fig. 3 where we have plotted the ratio of the real part of the conductivity in the superconducting state to that of the normal state $\sigma_{1S}(\omega)/\sigma_{1N}(\omega)$ as a function of frequency normalized to twice the zero temperature energy gap Δ_0. Note that all the curves start at $\omega/2\Delta_0=2$, i.e., at $4\Delta_0$, except for the BCS dirty-limit case[19] which, of course, starts at $2\Delta_0$ and is included only for comparison (solid curve starting at $2\Delta_0$). It is important to realize that the gap is to be cal-

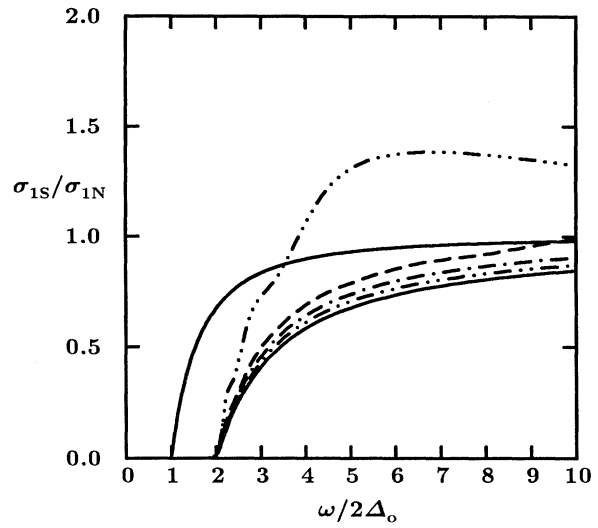

FIG. 3. The ratio of superconducting to normal state value of the real part of the conductivity $\sigma_1(\omega)$ as a function of frequency ω in units of twice the zero temperature energy gap Δ_0. The solid curve starting at $2\Delta_0$ is the BCS dirty limit and is shown for comparison. The curves all start at $4\Delta_0$ and apply to the clean limit ($t^+=0.0$). The solid curve is for a cutoff ω_c of 3000 meV while the others ending with the dashed-triple-dotted curve are for $\omega_c=1500$ meV, 600 meV, 400 meV, and 200 meV, respectively. Only the last (dashed-triple-dotted) curve, which corresponds to a gap ratio of $2\Delta_0/k_BT_c=8.2$, shows significant deviations from BCS in the Holstein region.

culated self-consistently. For a given value of Δ_0 the spectrum in Eq. (7) becomes gapped and this effect is included by replacing the lower limit for the integral on ω in (7) by $2\Delta_0$ rather than zero. After each run, the lower cutoff is readjusted until the value of Δ_0 no longer changes. The set of curves in Fig. 3 corresponds to a cutoff of 3000 meV (solid curve), 1000 meV (dashed-double-dotted curve), 600 meV (dashed-dotted curve), 400 meV (dashed curve), and 200 meV (dashed-triple-dotted curve), $2\Delta_0/k_BT_c$ values of 4.3, 4.7, 5.1, 5.7, and 8.2, respectively, and λ_ρ of 0.3, 0.6, 0.9, 1.5, and 6.4.

The observation from the figure, that, in all cases, the absorption in the clean limit starts at $4\Delta_0$ is consistent with the idea that absorption can only occur at $2\Delta_0$, the energy required to break a Cooper pair plus the lowest excitation energy for charge or spin fluctuations which also occur at $2\Delta_0$ in our model. This is reflected in the lower cutoff which we have applied self-consistently to the fluctuation spectrum. Note also that, even for an upper cutoff of 400 meV, a $\lambda_\rho=1.54$ with corresponding value of $2\Delta_0/k_BT_c=5.7$, the structure is small compared with its strength in a typical conventional strong-coupling system such as Pb. The reason for this is that our effective spectral density $\pi^{-1}\tanh(\omega/2T)$ is spread out over a large range of frequencies up to ω_c. Also the relatively large value of $2\Delta_0/k_BT_c$ which accompanies this spectrum is due, in part, to the application of a lower cutoff in (7) at $\omega=2\Delta_0$. This entirely cuts out low-lying charge and spin fluctuations with the effect that $2\Delta_0$ is larger relative to T_c than would be expected otherwise. The final curve (dashed-triple-dotted) in Fig. 3 is included only to show that Holstein processes can indeed become more visible when ω_c is made to be very low. In this case, $\omega_c=200$ meV and the curve behaves much more like a conventional strong-coupling system. We emphasize however that, when ω_c is not too small, the phenomenological charge-transfer resonance model of Refs. (7)–(11) can yield a large $2\Delta_0/k_BT_c$ without large Holstein structure. Kamarás *et al.*[3] and Schlesinger *et al.*[6] have noted that this is an essential feature of the data in Y-Ba-Cu-O which cannot be explained within the conventional formalism. As this, along with the fact that the absorption starts at $4\Delta_0$ in the clean limit, is one of our important results we emphasize it further in Fig. 4. In this figure we show the real part of $\sigma(\omega)$ in the superconducting state normalized to the normal state, $\sigma_{1S}(\omega)/\sigma_{1N}(\omega)$, for the case $2\Delta_0/k_BT_c=8.5$, $\lambda_\rho=5.27$, $g=0.5$, and $\omega_c=400$ meV (dashed line). It shows little structure at higher frequencies and does not deviate much in this energy range from the BCS dirty limit (solid curve). The second case, for which $2\Delta_0/k_BT_c=4.5$, $\lambda_\rho=1.25$, $g=0.8$, and $\omega_c=200$ meV (dashed-dotted curve), shows even less deviation from the solid curve in the Holstein region although the gap ratio and λ are not very different from the values for Pb which shows large deviations. This agrees with the experimental data.[3,6] To end we note that for both curves shown in Fig. 4 the structure around $\omega/2\Delta_0\simeq 5$ is due to our upper cutoff of the excitation spectrum and could presumably be smoothed out if a gradual cutoff had been used.

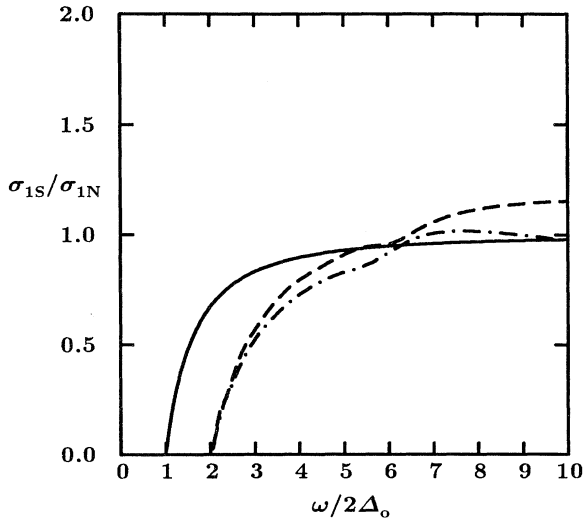

FIG. 4. The ratio of the real part of the conductivity in the superconducting state to its value in the normal state as a function of frequency in units of twice the zero temperature energy gap Δ_0. The solid curve is for comparison and applies to the dirty BCS limit. The dashed curve is for $2\Delta_0/k_BT_c=8.5$, $\lambda_\rho=5.27$, and $\omega_c=400$ meV with $g=0.5$, while the dot-dashed curve is for $2\Delta_0/k_BT_c=4.5$, $\lambda_\rho=1.25$, and $\omega_c=200$ meV with $g=0.8$. These curves start at $4\Delta_0$, since they apply to the clean limit, and show relatively small structure in the Holstein region when compared with a conventional strong-coupling superconductor.

In Figs. 5(a) and 5(b) we study the effect of ordinary impurities [finite value of t^+ in Eqs. (4) and (5)] on the ratio $\sigma_{1S}(\omega)/\sigma_{1N}(\omega)$. The four impurity concentrations used are $t^+=0.1$ meV (dashed curve), $t^+=1.0$ meV (dashed-dotted curve), $t^+=10.0$ meV (dashed-double-dotted curve), and $t^+=100.0$ meV(dashed-triple-dotted curve). The results are also compared with the pure case (solid curve). The most striking feature of these results is that as soon as impurities are introduced the absorption starts at $2\Delta_0$ rather than the $4\Delta_0$ found to occur in the pure case. The momentum can now be transferred to the impurity system. Some remnant of the $4\Delta_0$ threshold does, however, remain even in the $t^+=10.0$ meV curve which represents a large amount of impurities but is still far from the dirty limit.

It is of interest to consider the absolute value of the conductivity $\sigma_1(\omega)$ in the frequency range above the absorption edge. To do this the plasma frequency is adjusted to correspond to a value of the dc conductivity of 20 000 $(\Omega\,\mathrm{cm})^{-1}$ at 100 K in the normal state which is a typical value for the experimental samples. Since $\sigma_{1N}(\omega=0)$ goes like T in the marginal Fermi liquid, this corresponds to a dc conductivity at 10 K of 200 000 $(\Omega\,\mathrm{cm})^{-1}$. The normal state conductivity $\sigma_{1N}(\omega)$, as a function of frequency ω, is shown in Figs. 6(a) and 6(b) (dashed curve) for two illustrative model sets of parameters, namely, $2\Delta_0/k_BT_c=4.5$, $\lambda_\rho=1.25$, $g=0.8$, and $\omega_c=200$ meV [Fig. 6(a)] and $2\Delta_0/k_BT_c=5.1$, $\lambda_\rho=0.9$, $g=0.6$, and $\omega_c=600$ meV [Fig. 6(b)]. In the first case,

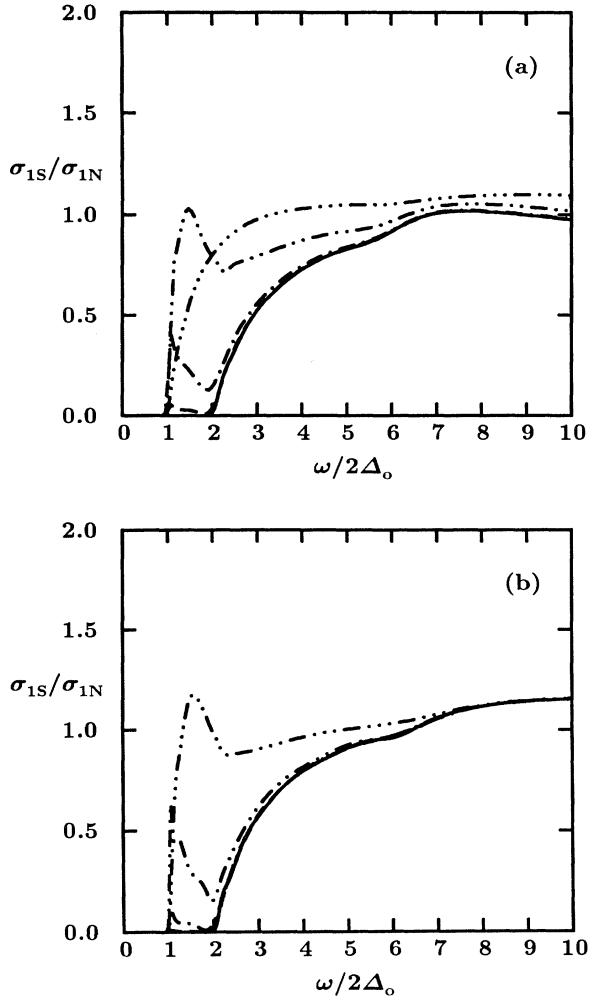

FIG. 5. The ratio of the real part of the conductivity in the superconducting state to its value in the normal state as a function of frequency in units of twice the zero temperature energy gap Δ_0. For the pure case (solid curve) the absorption starts at $4\Delta_0$ while when impurities are added the onset occurs at $2\Delta_0$ instead. Curves (a) are for the charge fluctuation model with $2\Delta_0/k_BT_c=4.5$ while curves (b) apply to the case $2\Delta_0/k_BT_c=8.5$ with other parameters defined in Fig. 4 and in the text.

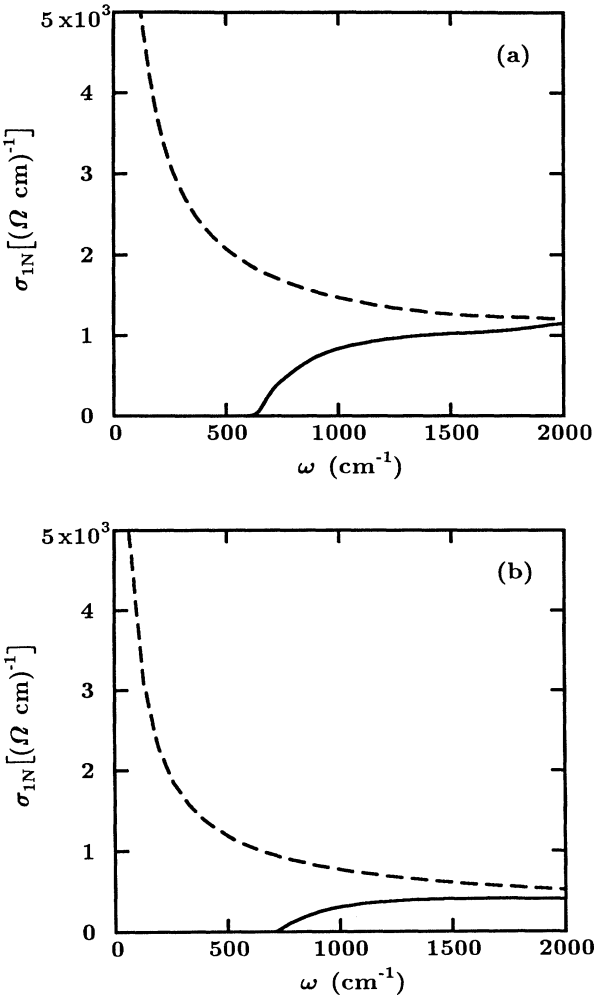

FIG. 6. The normal state (dashed curve) and superconducting state (solid curve) conductivity at 10 K for two sets of model parameters. The top frame is for $2\Delta_0/k_BT_c=4.5$, $\lambda_\rho=1.25$, $g=0.8$, and $\omega_c=200$ meV. The lower frame is for $2\Delta_0/k_BT_c=5.1$, $\lambda_\rho=0.9$, $g=0.6$, and $\omega_c=600$ meV. The plasma frequency has been chosen in both cases to obtain a value of $\sigma_{1N}(\omega=0)=20\,000\ (\Omega\,\mathrm{cm})^{-1}$.

the width at half maximum comes out to be $1.27k_BT$ and in the second it is $1.0k_BT$ which falls well within the range of experimental values.[3] Also shown for comparison are the corresponding values for $\sigma_1(\omega)$ in the superconducting state represented by the solid lines. We see that in the region around 2000 cm^{-1} the conductivity in one case is slightly above 1000 $(\Omega\,\mathrm{cm})^{-1}$ and, in the other, somewhat less than 500 $(\Omega\,\mathrm{cm})^{-1}$. These values are smaller, but of the same order of magnitude, as measured experimentally. Parameters could be varied to obtain better agreement with experiment if one wished. We do not think this to be appropriate at this time and in any case this is not our primary aim here. We believe that before a definitive comparison with experiment can be made it is important to calculate the complete temperature dependence of the conductivity in the superconducting state from T_c down to low T. In this way we could trace the opening up of the gap. Such a study would, however, require real-frequency-axis programs because Padé approximants are not reliable at high T near T_c. Nevertheless, we can make two statements about experiments. The amount of absorption calculated in the mid-infrared region for the marginal Fermi-liquid model is of the same magnitude but smaller than the amount observed and therefore leaves some room for extra absorption processes not accounted for in the model. If this is the case, it might be very hard to see a clear gap in such experiments particularly if one is in the clean limit. Undoubtedly some residual resistivity needs to be added according to sample quality but the amount is not unambiguously known at this point. A very nice feature of the theory is that the dc conductivity scales like $1/T$ with coefficients in front of this variation dependent on the single remaining parameter of the model for a given cutoff.

V. CONCLUSIONS

We have calculated the superconducting and low temperature normal state finite frequency conductivity using an imaginary-axis formulation of the current-current correlation function with Padé approximants to perform the necessary final analytic continuation to get $\sigma(\omega)$ for real frequencies ω. Comparison with recent results obtained with the same technique reveals a discrepancy in the pure limit but good agreement for finite mean free paths. Also, in the one case tried, our results are in excellent agreement with those obtained by Lee *et al.*[4] using a real-frequency-axis formulation of the problem. This alternate technique is very different mathematically and numerically from the one adopted in this work. The excellent agreement gives striking evidence for the validity of both numerical techniques.

In the prominently studied phenomenological charge-transfer resonance model summarized by Varma,[7] there is coupling to charge as well as spin degrees of freedom. In the simplest versions of the theory, the excitation spectrum for both charge and spin fluctuations are the same but have different coupling strength to the superconducting electrons. An important feature of the theory is that this spectrum extends over a large energy range up to ω_c which could be as large as a few thousand meV. Also, as the gap in the quasiparticle excitations opens up, the fluctuation spectrum is to be cut off below $2\Delta_0$. We have studied the behavior of $\sigma(\omega)$ for a model with the above features and found several important results. First, in the pure limit, absorption can start only at $4\Delta_0$ which is the energy required to form a quasiparticle pair plus the lowest energy in the fluctuation spectrum. When impurities are added, momentum can go into the impurity system, and the absorption starts at $2\Delta_0$. For low impurity concentrations a remnant of the $4\Delta_0$ threshold remains prominent but eventually disappears when t^+ is large enough. Compared with a conventional electron-phonon model, the charge-transfer resonance model can produce relatively large values for the gap to critical temperature ratio with small associated Holstein structure as required in the experimental data.[3,6] The reason for this is twofold. First, the corresponding electron-boson spectral density is spread out over a large frequency range when the value of the cutoff in the fluctuation spectrum (ω_c) is large. Second, the fluctuations become gapped at low frequencies quenching both spin and charge degrees of freedom in this region. This has the net effect of increasing Δ_0 over the value that would be expected if no low energy cutoff was applied.

Finally, when the absolute value of the conductivity is fixed to the measured normal state value at $\omega=0$ [20 000 $(\Omega\,\mathrm{cm})^{-1}$ typically], with the width at half maximum of $\sigma_{1N}(\omega)$ of the observed order, $1.0-1.5k_BT$, its weight in the mid-infrared region is of the same order of magnitude as is observed although, in all the cases considered, it is smaller. This leaves room for some additional absorption process in this region which would add to the direct electronic contribution calculated in this paper. While we have not attempted a close comparison with experiment, the model does reproduce many of the observed features.

In the future we plan to implement a real-frequency-axis formulation of the conductivity. This will allow us to calculate $\sigma_1(\omega)$ at any temperature and in particular study how the gap opens up as a function of temperature in the range T_c to 0 K. We will then attempt a more detailed comparison with the experimental data.

It has been brought to our attention that Littlewood and Varma have recently performed similar calculations.[20]

ACKNOWLEDGMENTS

This work was partly supported by the Natural Sciences and Engineering Research Council of (NSERC) of Canada and by the Canadian Institute for Advanced Research (CIAR). We appreciated correspondence with Dr. N. E. Bickers.

[1]T. Timusk and D. B. Tanner, in *Physical Properties of High Temperature Superconductors I,* edited by D. M. Ginsberg (World Scientific, Singapore, 1989), p. 339.

[2]Z. Schlesinger, R. T. Collins, F. Holtzberg, C. Field, G. Koren, and A. Gupta, Phys. Rev. B **41**, 11 237 (1990).

[3]K. Kamarás, S. L. Herr, C. D. Porter, N. Tache, D. B. Tanner, S. Etemad, T. Venkatesan, E. Chase, A. Inam, X. D. Wu, M. S. Hegde, and B. Dutta, Phys. Rev. Lett. **64**, 84 (1990).

[4]W. Lee, D. Rainer, and W. Zimmermann, Physica C **159**, 535 (1989).

[5]N. E. Bickers, D. J. Scalapino, R. T. Collins, and Z. Schlesinger, Phys. Rev. B **42**, 67 (1990).

[6]Z. Schlesinger, R. T. Collins, F. Holtzberg, C. Field, N. E. Bickers, and D. J. Scalapino, Nature (London) **343**, 242 (1990).

[7]C. M. Varma, Int. J. Mod. Phys. B **3**, 2083 (1989).

[8]C. M. Varma, P. B. Littlewood, S. Schmitt-Rink, E. Abrahams, and A. Ruckenstein, Phys. Rev. Lett. **63**, 1996 (1989).

[9]C. M. Varma, S. Schmitt-Rink, and E. A. Abrahams, Solid State Commun. **62**, 681 (1987).

[10]P. B. Littlewood, C. M. Varma, S. Schmitt-Rink, and E. A. Abrahams, Phys. Rev. B **39**, 12 371 (1989).

[11]Y. Kuroda and C. M. Varma, Phys. Rev. B **42**, 8619 (1990).

[12]J. M. Daams, B. Mitrović, and J. P. Carbotte, Phys. Rev. Lett. **46**, 65 (1981).

[13]R. Baquero, J. M. Daams, and J. P. Carbotte, J. Low Temp. Phys. **42**, 585 (1981).

[14]H. G. Zarate and J. P. Carbotte, J. Low Temp. Phys. **57**, 291 (1984).

[15]J. M. Daams and J. P. Carbotte, J. Low Temp. Phys. **43**, 263 (1981).

[16]D. Rainer and G. Bergmann, J. Low Temp. Phys. **14**, 501 (1974).

[17]H. J. Vidberg and J. W. Serene, J. Low Temp. Phys. **29**, 179

(1977); and private communication with N. E. Bickers.
[18]D. J. Scalapino, in *Superconductivity,* edited by R. D. Parks (Marcel Dekker, New York, 1969), p. 449.
[19]D. C. Mattis and J. Bardeen, Phys. Rev. **111**, 412 (1958).
[20]P. B. Littlewood and C. M. Varma, in Proceedings of the International Seminar on Theory of High-T_c, Dubna, USSR, 1990 (to be published).